Measuring Techniques for Transonic and Supersonic Flow in Cascades and Turbomachines

13th Symposium
September 5-6, 1996

ETH Zürich
Institute of Energy Technology
Turbomachinery Laboratory

HETERODYNE LASER INTERFEROMETRY FOR CASCADE FLOW INVESTIGATIONS

Jakob Woisetschläger Herbert Jericha

Institute for Thermal Turbomachinery and Machine Dynamics
Technical University Graz, Inffeldgasse 25, A- 8010 Graz, Austria

Phone: +43 316 873 7229; Fax: +43 316 873 7234
eMail: TTM @TTM.TU-GRAZ.AC.AT

ABSTRACT

Currently, in two ongoing projects funded by the Austrian Science Foundation experiments are performed in the institute's transonic cascade. For these experimental tests different laser techniques - Laser Doppler Anemometry, Holographic Interferometry and Differential Interferometry - have been used together with various kinds of standard diagnostic techniques (For flow investigations the Institute for Thermal Turbomachinery and Machine Dynamics is equipped with a 3MW compressor station located in the two basements of the institute). Here we present our results obtained with digitally evaluated interferometric techniques. Whereas holographic interferometry was used for subsonic flow diagnostics, differential interferometry provided quantitative data on density gradients in transonic flows.

1.Introduction:

From 1994 to 1999 six institutes from the two Austrian Technical Universities Graz and Vienna participate in the Research Program S68 "Thermal Energy Production-Efficiency Improvement and Emission Reduction of Thermal Power Plants" led by H.Jericha. This Research Program tackles the problem of efficiency improvement on several fronts. Some of the projects deal with materials for high temperature steam plants, gas turbines for particle loaded gases, efficiency improvement by cycle optimisation and flow optimisation in turbomachinery. Many of the results obtained during the first two years have been published at ASME Cogen Turbo Conference 1995 in Vienna.

For the enhancement of the accuracy of computational fluid dynamics methods, the projects are supported by data acquisition in a transonic test rig at the institute and will be supported by data from a continuously operating test turbine currently under construction. For this purpose the laboratory at the Institute for Thermal Turbomachinery and Machine Dynamics is equipped with a 3MW compressor station located in the two basement of the institute. This compressor station consists of one screw and two turbo compressors and can operate in 13 different configurations with pressure ratios between 3 up to 10 and mass flows from 2.5 up to 15 kg/s [1]. One of the test rigs currently used for the research program is the transonic cascade - a linear arrangement of seven blades (each with a height of 10cm) with a window section on both sides to enable the use of non-intrusive optical methods. Among those are colour Schlieren visualisation, Laser-Doppler-Velocimetry for velocity measurements along grid coordinates provided by the numerical flow calculations and interferometric methods. Since large amounts of numerical data are needed for numerical code improvement there is a need for a digital evaluation of interferograms to obtain density information from subsonic or transonic flows. This is of special importance since in turbulent flows interferograms recorded with a pulsed laser system give only momentary density information, but density maps of flow fields should represent mean values. Different techniques for fringe evaluation had been developed since more than 10 years by several authors [2,3,4,5,6,7]. In the following we will present and discuss techniques for heterodyne holographic and heterodyne differential interferometry we use in our test rigs.

2. Holographic Interferometry
Temporal Heterodyning (Phase Stepping)

Fig. 1 shows a typical holographic interferogram of a transonic flows through our linear blade cascade recorded with a pulsed ruby laser (LUMONICS HLS2). The optical setup was mounted on a table equipped with vibration insulation and was shielded with a cover against the acoustic noise from the continuously operated test rig. Since the interferogram was recorded with and without flow the interference lines represent isolines of flow density. The interferogram was digitised using a Hitachi KP-110 CCD camera and a PC Vision Plus frame grabber

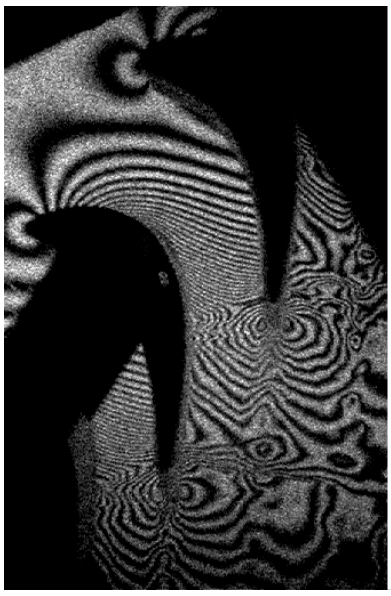

Fig.1 pulsed holographic interferogram of transonic flow at isentropic exit Mach number M= 1. The blade chord length was 58 mm.

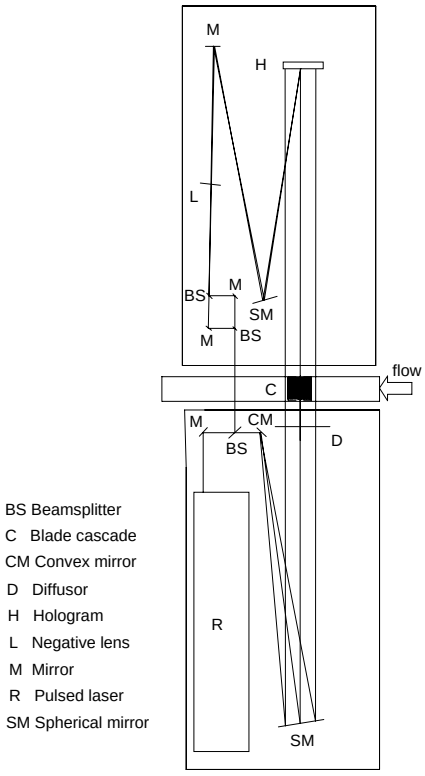

Fig.2. Setup for two reference beam recording of holographic interferograms at the institute's turbine blade cascade

board in a 486 PC with a 512 x 512 pixel resolution. The intensity along a line in this digitised interferogram is now given by

$$I(x,y) = I_0(x,y) + M(x,y) \cdot \cos \Delta \phi (x,y) \quad , \tag{1}$$

with x and y the coordinates within the interferogram, $I_0(x,y)$ the background intensity (e.g. caused by the illumination) and as second term the interference fringes $\cos\Delta\phi(x,y)$ with their modulation $M(x,y)$ and the phase shift $\Delta\phi$ between the two holographically recorded wavefronts. This phase shift was caused by the density change $\rho(x,y)$ within the cascade:

$$\phi(x,y) = 2\pi \Delta z \frac{K\rho(x,y)+1}{\lambda} \tag{2}$$

with K the Gladstone Dale constant for air (see e.g. [9,10]), Δz the blade height (channel height) and λ the wavelength of the laser light (694 nm for ruby, 633 nm for Helium-Neon laser).

Temporal heterodyning now uses two reference beams for recording the holographic interferogram [5,6] (see Fig.2). These reference beams meet at the plane of the hologram under a very narrow angle and were in our case produced by a small Mach-Zehnder interferometer (100 times 100 mm square, see Fig.2). Both reference beams then produced a spurious fringe system of about 0.5 mm fringe spacing in the plane of the hologram. (For the alignment we used a Helium-Neon laser, the quality of the two reference beams superposition was then controlled in a first test recording with the pulsed laser). Since it also helps to improve digital evaluation we used collimated reference beams.

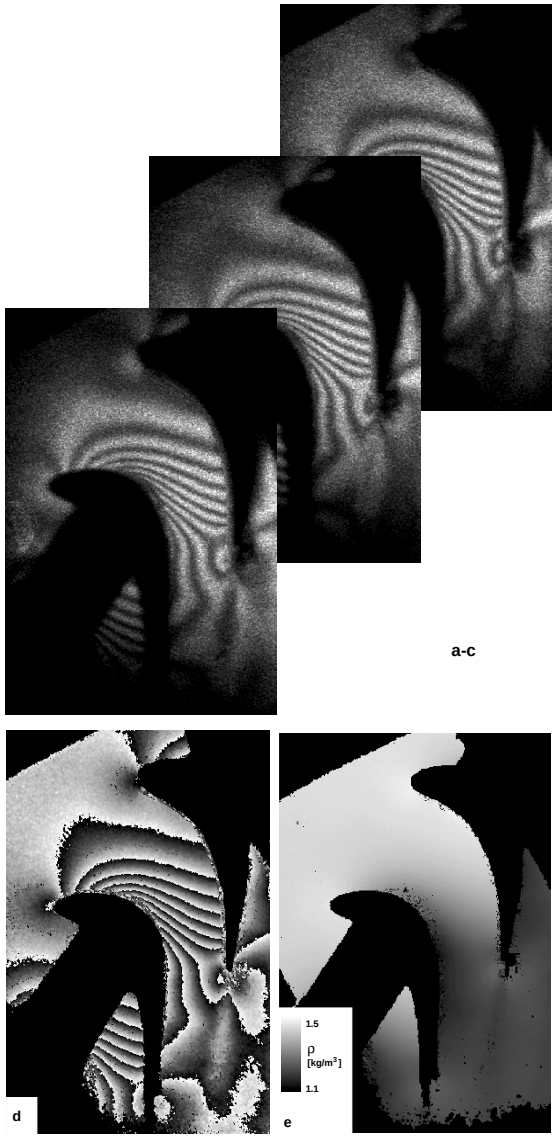

Fig.3 Phase stepped holographic interferogram of subsonic flow at exit Mach number M=0.6 a-c)three phase stepped images (120° phase steps) d) modulo 2π reconstruction of interference fringes e) density map

One reference beam was then used for the first, the other reference beam for the second holographic recording. This alternating blockage of the beams can be done by a standard beam shutter when there is enough time between the two exposures. In the case the pulsed ruby laser is used in the double pulse mode with a few μs delay time between the pulses we use a STEINBICHLER acousto-optical modulator unit and a trigger electronic which switches the reference beams between the two pulses with an acousto-optical modulator providing the two reference beams.

For the reconstruction of such holograms recorded with two reference beams we used a 690nm laser diode (LASER 2000, 30mW) and exactly the same setup as for recording, except that in one reference beam one of the mirrors was now mounted on a piezoelectric transducer. During reconstruction the mirror can so be shifted step-wise thus adding a constant phase-shift to the interferogram (see Fig3.a-c, phase-steps of 120° were applied between the three image recordings). The desired phase distribution $\Delta\phi(x,y)$ is calculated from

$$\phi(x,y) = tan^{-1}\left(\frac{\sqrt{3}(I_3(x,y) - I_2(x,y))}{2I_1(x,y) - I_2(x,y) - I_3(x,y)} \right) \quad (3)$$

with $I_{1,2,3}$ the intensity distributions in the three phase stepped interferograms.

Due to the ambiguity of the arctan function a so called "modulo 2π" - function results (Fig.3d) where the phase jumps have to be detected and removed [7,8]. The result for the subsonic cascade flow is given in terms of density in Fig.3e.

Different phase stepping algorithms exist (we use three step, four step, six plus one step, Carré) with their advantages and disadvantages discussed in literature [4,6,7]. Main errors inherent in this evaluation are precision and calibration errors in the phase stepping device. One possible way to check for these errors is to place the reconstruction setup on a vibrational insulated table covered against free air convection. Then two measurement on the same interferogram are taken and substracted. For well calibrated system the error can be in the size of 1/100 of a wavelength.

3.Holographic Interferometry - Spatial Heterodyning (Fourier Analysis)

For real time observation (e.g. in high speed mode) and continuous recording of interferograms on tape or digital storage another technique widely used had proven useful. For this spatial heterodyning a parallel fringe system is heterodyned to the interferogram (see Fig. 4a,b; the heterodyning can be performed by tilting a mirror in the reference beam between the to holographic exposures; see also Fig.5). In this way a linear phase shift is superimposed to the phase shift caused by the density change (see eq.2). An interferogram of this type (Fig.4b) enables a Fourier analysis of the digitised images.

Using Euler identity eq.1 can be written as

$$I(x,y) = I_0(x,y) + G(x,y) + G^*(x,y) \quad (5)$$

with

$$G(x,y) = 1/2\, M(x,y)\, exp[+i\Delta\phi(x,y)] \quad (6a)$$

and

$$G(x,y)^* = 1/2\, M(x,y)\, exp[-i\Delta\phi(x,y)] \quad (6b)$$

the real and imaginary part of the interference signal. Now a Fast Fourier Transform is performed on the signal $I(x,y)$ resulting in $i(\nu_x,\nu_y)$, the intensity distribution in the Fourier domain,

$$i(\nu_x,\nu_y) = i_0(\nu_x,\nu_y) + g(\nu_x,\nu_y) + g^*(\nu_x,\nu_y) \quad (7)$$

with ν_x,ν_y the spatial frequencies in x and y direction respectively.

Due to the heterodyning process in the spatial domain (superposition of the high frequency carrier fringe system) the signal containing the interferometric information G(x,y) is now shifted towards the high frequency range in the Fourier domain. In the Fourier domain the signal $g(\nu_x,\nu_y)$ needed for the reconstruction of the phase or density information is so clearly separated from the low frequency background and modulation noise $i_0(\nu_y)$ (see Fig.4c, zero order low frequency noise in the center, +1 and -1 order containing the signal $g(\nu_x,\nu_y)$ and its conjugate $g^*(\nu_x,\nu_y)$ on each side; additionally a second order signal and its conjugate is visible caused by the nonlinear recording of the sinussoidal fringes by the CCD sensor). A rectangular window with the full width $2\Delta\nu$ is now applied to the Fourier domain filtering only the signal $g(\nu_x,\nu_y)$ and

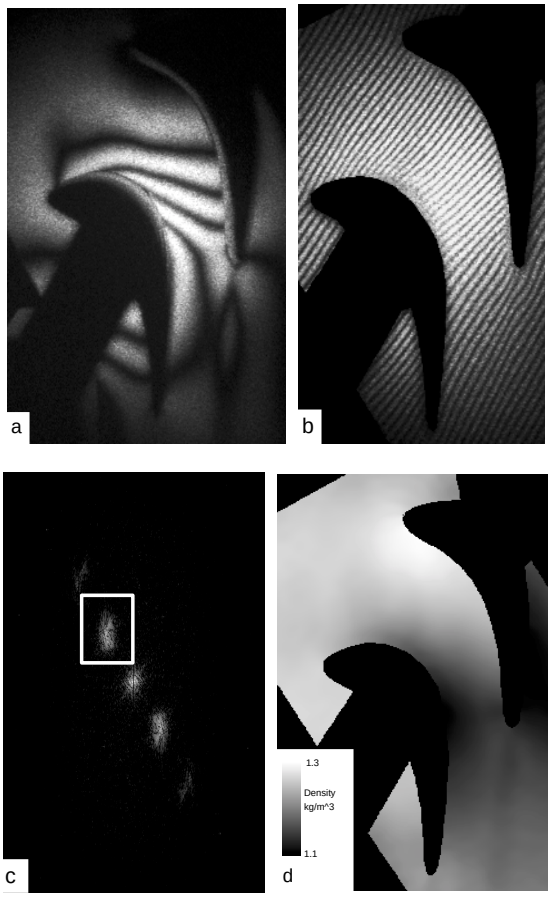

Fig. a) Holographic interferogram of subsonic flow without and b) same interferogram with carrier fringe system heterodyned c) frequency spectrum of b) with window for filter process d) resultant density map

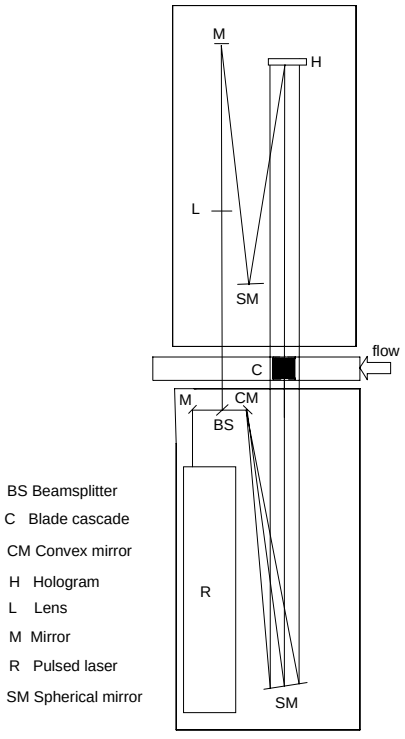

Fig.5 Setup for spatial heterodyne holographic interferometry

setting the other frequencies to zero. This filtered spectrum is then subject to a back transformation to the spatial domain. The phase distribution in the wavefront is so calculated from the filtered signal in the spatial domain

$$\Delta\phi(x) = \arctan\frac{Im(G(x))}{Re(G(x))} \tag{8}$$

(Again the phase ambiguity in eq.8 has to be removed.)

In this phase distribution the heterodyned carrier fringe system still dominates with its linear increase in phase. This linear phase distribution could be compensated by performing a linear regression with following substraction of this linear term. We actually used another way of compensation in recording a reference interferogram without flow. This reference interferogram not only contains the linear phase increase of the carrier fringe system, but also all distortion within the optical path, e.g Schlieren in the window or a not exactly (in an interferometric dimension) plane wavefront.

The final result of this substraction of a reference phase recording from the flow recording is shown in Fig.4d already in terms of density.

The errors inherent to the filtering process are best judged in the Fourier domain as given in Fig.4c. By the mean signal height in the rectangular window used for signal reconstruction and the mean noise level the error in phase measurement $\Delta(\Delta\phi(x,y))$ can be calculated by using the signal over noise ratio SNR [8].

$$\Delta(\Delta\phi) = \frac{1}{\sqrt{SNR}}\frac{\sqrt{SNR}+1}{\sqrt{SNR}-1} \tag{9}$$

The spatial resolution in the final reconstruction can also be derived from the frequency spectrum using the Nyquist theorem and the window width $2\Delta\nu$ used for reconstruction

$$D = \frac{1}{2\Delta\nu} \tag{10}$$

with D the smallest distance correctly sampled. Smaller structures could be resolved either by increasing the frequency of the carrier fringe system and eventually by zooming into the field.

4.Heterodyne Differential Interferometry

Differential interferometry is a technique used to measure density gradients in flows [9,10].In our case this is done by using one parallel beam of light running through the test zone and then through a small interferometer (Fig.6). This small interferometer allows not only adjustment of sensitivity but also to heterodyne a carrier fringe system independently from the shear in order to use a Fast Fourier Transform for fringe evaluation.

Within this interferometer this wavefront is sheared against itself (for clarity we will here assume a shear Δy in y direction only). At the exit of the interferometer each light beam interferes with a neighbouring at a distance Δy. This interferometer detects the density gradient within a flow according to

$$\frac{\Delta\phi(x,y)}{\Delta y} = \frac{\phi(x,y-\Delta y/2)-\phi(x,y+\Delta y/2)}{\Delta y} \approx 2\pi\Delta z\frac{K}{\lambda}\frac{\partial\rho(x,y)}{\partial y} \tag{11}$$

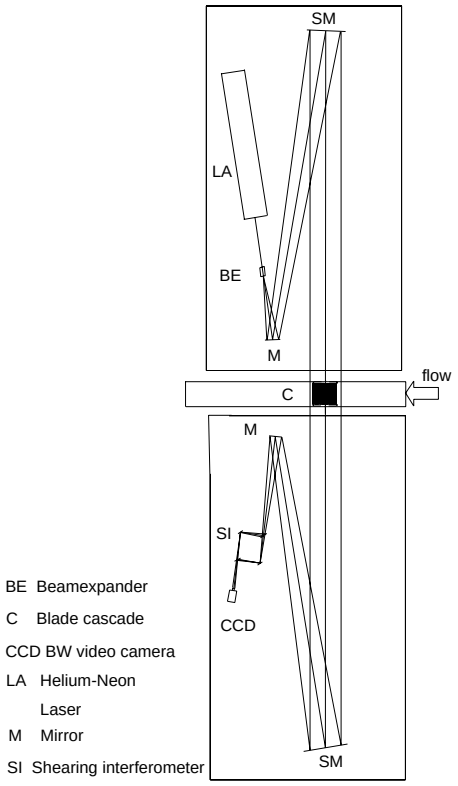

Fig.6 Setup for heterodyne differential interferometry

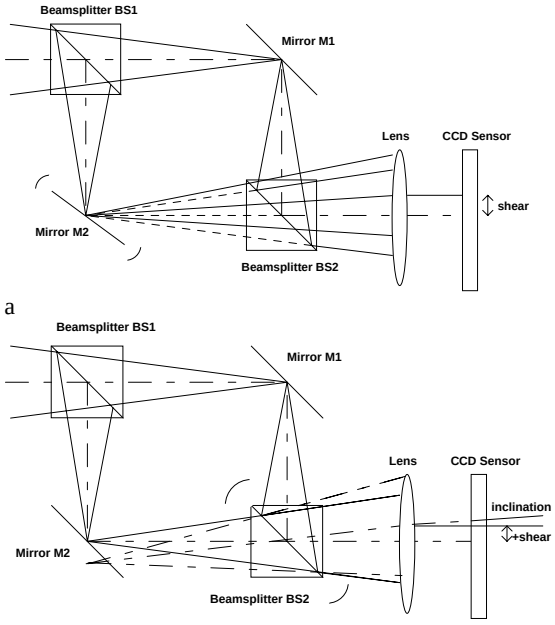

Fig.7 Shearing interferometer for heterodyne differential interferometry a) adjustment of shear b) adjustment of inclination (Carrier fringe system)

(same will be valid for a shear in x direction) [9,10].

By changing the shear this type of interferometer has an adjustable sensitivity. The experimentalist can choose sensitivity either for shock or boundary layer investigations.

Basically the setup is a Schlieren setup with a small Mach-Zehnder interferometer instead of the Schlieren stop

Fig.8 Real time shock visualisation using a carrier fringe system perpendicular to the shear direction (differential interferometry)

[12]. Figs.7a,b show this interferometer in all details. The laser light wave is split by beamsplitter BS 1 into two parts with both light fronts focused on the mirrors M1 and M2 by the spherical mirror in the Schlieren setup. By tilting one of the mirrors (here mirror M2; Fig.7a) the wavefronts (again superimposed by beamsplitter BS2) can be sheared against each other. To heterodyne a carrier fringe system beamsplitter BS2 has to be tilted, adding a shear and an inclination to the wavefronts (Fig.7b). While the additional shear can be compensated for by tilting the mirror M2 in opposite direction, the inclination will produce the desired carrier fringe system. The direction of the carrier fringe system can be perpendicular to the shear for shock detection and visualisation (see Fig.8; recorded with a KODAK EKTAPRO 1000 high speed camera) or parallel to the shear (Fig.9a; recorded with a Hitachi standard CCD camera) for Fourier Analysis.

The evaluation of an heterodyned differential interferogram as given in Fig.9.a is identical to the evaluation of spatially heterodyned holographic interferograms (see section 3 above). Again the frequency spectrum (Fig.9b) is filtered, the modulo 2π map calculated (Fig.9c), unwrapped and a reference recording without flow substracted. This reference recording not only compensates for the carrier fringe system (the linear phase) but also for all wavefront distortion, e.g. caused by Schlieren in the windows. The final result is given in Fig.9d.

5.Discussion

For holographic interferometry a special shielding against vibration and acoustic excitation is necessary. Fig.10 gives the acoustic pressure caused by our transonic cascade on an element in 1m distance to the continuously operated cascade with and without shielding against airborne vibration. This shielding together with a vibration insulation (we used Newport I2000 active vibration insulators) is absolutely essential for holographic interferometry.

In heterodyne differential interferometry only the interferometer part had to be shielded. For this purpose the interferometer (dimensions 100x100 mm) had been set up on a 2 cm thick steel plate standing on three steel balls. There was no other vibration insulation. The observation through this differential interferometer is possible in real time (Fig.8 is a high speed recording of the shock oscillations).

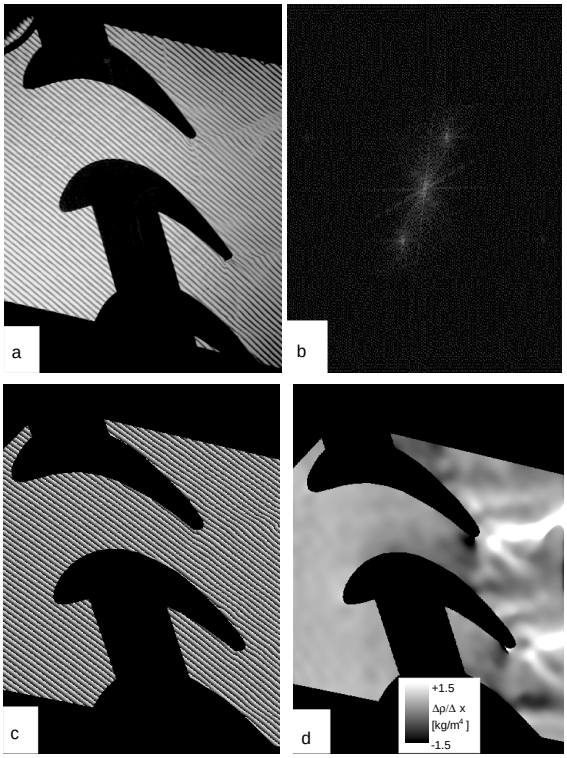

Fig.9 a) Heterodyne differential interferogram, b) frequency spectrum, c) modulo 2π phase map, d) density gradient map

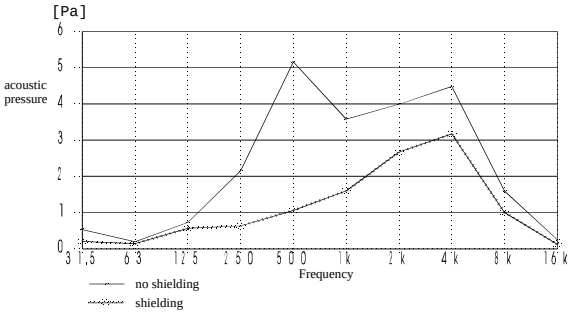

Fig.10 Sound pressure on an optical element caused by the continuously running cascade with and without shielding of the optical setup.

While heterodyne differential interferometry is highly insensitive to noise and therefore can be used even under harsh conditions, two errors contribute to the result. One is the error caused by the digital evaluation in the frequency domain discussed in section 3 above. Here the spatial resolution is given by the window width in the frequency domain and the error in the phase map is caused by the signal to noise ratio. Secondly, for calculating the density gradient an exact value for the shear is necessary (see eq.11 above). This shear can be measured in the camera image by placing an object in the test zone and detecting the image shift in the CCD plane (together with a length calibration in the image), or by measuring the tilting angle of the beams after the interferometer by using unexpanded laser beams. While the relative error within the field is usually in the order of a few percent, the absolute error in density gradient might be up to 10% what is more than in the other techniques detecting density changes.

In transonic flow field investigations the shock area is most critical due to the high sensitivity of interferometric techniques. Additionally in spatial heterodyne interferometry the carrier fringe frequency has to be significantly higher than the modulation frequency to obtain a high enough shift in the frequency domain. Therefore a compromise has to be found for shock areas. In heterodyne differential interferometry this can be compensated for by its adjustable sensitivity.

Summary

Three different interferometric techniques had been introduced the way they are used at the Institute for Thermal Turbomachinery and Machine Dynamics for flow diagnostics. All three techniques produce digital maps of density or density gradients, thus enabling compensation for wavefront distortions by substracting of reference recordings as well as averaging of density maps recorded in single interferograms.

Acknowledgement

The authors gratefully acknowledge the support by the Austrian Science Foundation (FWF) in supporting ongoing research in efficiency improvement of thermal power plants.

References

[1] P.Pirker, H.Jericha, G.Zhuber-Okrog (1995) Auslegung und Betrieb einer Verdichteranalge für die Luftversorgung wissenschaftlicher Versuchseinrichtungen, VDI Berichte 1208, 331-347

[2] Kreis T (1996) Holographic interferometry, Berlin: Akademie Verlag

[3] Takeda M; Ina H; Kobayashi K (1982) Fourier-transform method of fringe pattern analysis for computer-based topography and interferometry. J.Opt.Soc.Am.72: 156-160

[4] Kreis T (1986) Digital holographic interference-phase measurement using the fourier-transform method. J.Opt.Soc.Am.A 3: 847-855

[5] H.Dändliker, R.Thalmann (1985) Heterodyne and quasi-heterodyne holographic interferometry , Opt.Eng. 24: 824 - 831

[6] K.Creath (1988) Phase-measurement interferometry techniques, In: Progress in Optics (ed. E.Wolf) XXVI, Elvesier Science Publisher

[7] W.Osten (1991) Digitale Auswertung von Interferenzbildern, Berlin, Akademie Verlag

[8] Vukicevic D; Neger T; Jäger H; Woisetschläger J; Philipp H (1990) Optical tomography by heterodyne holographic interferometry. In: Holography (ed. Greguss P; Jeong T H) IS9, pp 160-161, Bellingham, Society of Photo-Optical Instrumentation Engineers

[9]Oertel H sen.; Oertel H jun. (1989) Optische Strömungsmeßtechnik. pp 337-64, Karlsruhe: G.Braun

[10] W.Merzkirch (1987), Flow Visualisation, Orlando, Academic press

[11] J.Woisetschläger, G.Pretzler, N.Mayrhofer, H.P.Pirker, H.Jericha , Heterodyne differential interferometry for turbine blade cascade flow investigations, submitted to Exp.Fluids

[12] G.Pretzler, H.Jäger, T.Neger, (1993) "High-accuracy differential interferometry for the investigation of phase objects", Meas.Sci.Technol., 4, 649-658